Available online at www.sciencedirect.com
SCIENCE DIRECT®
Biochimica et Biophysica Acta 1615 (2003) 1–6
BIOCHIMICA ET BIOPHYSICA ACTA
BBA
www.bba-direct.com

Rapid report

Atomic force microscopy studies of interaction of the 20S proteasome with supported lipid bilayers

Shou Furuike[a], Junya Hirokawa[b], Shinpei Yamada[b], Masahito Yamazaki[a,c,*]

[a] *Division of Materials Science, Graduate School of Science and Engineering, Shizuoka University, Shizuoka 422-8529, Japan*
[b] *Department of Biology, Faculty of Science, Shizuoka University, Shizuoka 422-8529, Japan*
[c] *Department of Physics, Faculty of Science, Shizuoka University, Shizuoka 422-8529, Japan*

Received 24 June 2003; received in revised form 17 July 2003; accepted 17 July 2003

Abstract

The 20S proteasome plays important roles in degradation of intracellular proteins. Mechanisms of its activation, its localization in cells, and its binding to biomembranes are not well understood. In this study, we used atomic force microscopy (AFM) to investigate interactions between the 20S proteasome and supported bilayers of various lipids in a buffer. We found that the 20S proteasome specifically bound to supported bilayers containing phosphatidylinositol (PI), but did not bind to supported bilayers containing phosphatidylcholine, phosphatidic acid or dioleoyltrimethylammonium propane. Binding of the 20S proteasomes had a high orientation; almost all were in a top view position. The specific and orientational binding of the 20S proteasome with PI may play important roles inside cells such as endoplasmic reticulum (ER) membrane. Use of AFM to study supported bilayers provides new information on ligand–receptor interactions.

Keywords: Supported lipid bilayer; Atomic force microscopy; 20S proteasome; Phosphatidylinositol; Endoplasmic reticulum (ER)

In eukaryotic cells, degradation of most intracellular proteins is catalyzed by the 26S proteasome (2.5 MDa) [1,2]. The proteins degraded by the 26S proteasome include short-lived regulatory proteins, as well as misfolded newly synthesized proteins translocated into the endoplasmic reticulum (ER) membrane [3,4]. It is generally thought that 26S proteasomes are located in the cytosol and at the ER membrane [5]. The 26S proteasome is composed of the 20S proteasome (700 kDa), which has peptidase activity, and two 19S regulatory complexes that include six ATPases and 11 or more non-ATPase subunits [6]. The three-dimensional structures of 20S proteasomes from *Thermoplasma acidophilum* [7], budding yeast [8] and bovine liver [9] have been determined by X-ray diffraction analysis of their crystals, and these structures appear to be highly conserved. The 20S proteasome has a hollow cylindrical structure composed of four stacked rings (α-β-β-α), each of which is composed of seven α subunits or seven β subunits. The 19S regulatory complexes can bind to the ends of the 20S proteasome; i.e., at the two α-rings.

The peptidase activities of the 20S proteasome are essentially latent, and several factors (such as cardiolipin, fatty acid, divalent cations [e.g., Mn^{2+}] and SDS) are activators of the 20S proteasome [10–14]. However, the mechanisms of activation by these substances are not understood. Clarification of these mechanisms requires observation of structural changes in the 20S proteasome induced by these substances in a buffer. On the other hand, it is thought that the 20S proteasome can bind to biomembranes such as ER and other subcellular organelles [5]. Ubiquitination of misfolded proteins is performed at the ER membrane; thus, it is reasonable to hypothesize that the 20S proteasome is localized at (or near) the ER membrane. However, the mechanism of its localization is not well understood. Electron microscopic examination has shown that the human 20S proteasome binds with a specific

Abbreviations: AFM, atomic force microscopy; DPPC, 1,2-dipalmitoyl-*sn*-glycero-3-phosphatidylcholine; SOPC, 1-stearoyl-2-oleoyl-*sn*-glycero-3-phos-phatidylcholine; DOPA, 1,2-dioleoyl-*sn*-glycero-3-phosphatidic acid; DOTAP, 1,2-dioleoyl-3-trimethylammonium propane; PI, phosphatidylinositol; Lα phase, liquid-crystalline phase

* Corresponding author. Department of Physics, Faculty of Science, Shizuoka University, 836 Oya, Shizuoka 422-8529, Japan. Tel./fax: +81-54-238-4741.
E-mail address: spmyama@ipc.shizuoka.ac.jp (M. Yamazaki).

0005-2736/$ - see front matter © 2003 Elsevier B.V. All rights reserved.
doi:10.1016/S0005-2736(03)00227-X

orientation to phosphatidylinositol (PI) monolayer membrane, but it binds randomly to other lipid monolayer membranes such as PC (phosphatidylcholine) and PA (phosphatidic acid) [15]. This suggests that the 20S proteasome can bind to the PI membrane, but it is difficult to determine whether it can bind to other lipid membranes such as PC and PA, due to artifacts from sample preparation for electron microscopy (such as staining with uranyl acetate and air-drying). Thus, other experimental methods are needed to examine binding of the 20S proteasome to lipid membranes in a buffer.

Recent studies have shown that atomic force microscopy (AFM) can detect static and dynamic structures of proteins and lipid membranes in water [16–19]. In the AFM method, drying of samples and staining with heavy metals such as uranyl acetate are not necessary. Moreover, it is potentially possible to observe structural changes in proteins induced by substances in water in situ [20]. To observe structures of proteins in water at a high resolution, it is essential to prepare two-dimensional crystals [17,21]. For this purpose, it is necessary to find a lipid that can bind to a protein specifically.

In this study, we used AFM to investigate interactions of the 20S proteasome from bovine red blood cells on supported bilayers of various lipids in a buffer. We found that the 20S proteasome can specifically and strongly bind to lipid membranes containing PI in the buffer. We observed, with relatively high resolution, that the 20S proteasomes bound to these membranes in a top view position. Part of this study was presented at the 40th Annual Meeting of the Biophysical Society of Japan [22].

The following chemicals were purchased from Avanti Polar Lipids Inc. (Alabaster, AL, USA): 1,2-dipalmitoyl-*sn*-glycero-3-phosphatidylcholine (DPPC), 1-stearoyl-2-oleoyl-*sn*-glycero-3-phos-phatidylcholine (SOPC), 1,2-dioleoyl-*sn*-glycero-3-phosphatidylcholine (DOPC), 1,2-dioleoyl-*sn*-glycero-3-phosphatidic acid (DOPA), and 1,2-dioleoyl-3-trimethylammonium propane (DOTAP). PI from bovine liver was purchased from Sigma-Aldrich Japan K.K. (Tokyo, Japan). Ruby mica (10×10 mm; thickness, 300 ± 20 μm) was purchased from S&J Trading Inc. (Glen Oaks, NY, USA).

The 20S proteasomes were purified from bovine red blood cells by sequential chromatography using a Q Sepharose, Sephacryl S-400, Phenylsepharose, and Resource Q column, essentially as described previously by Ma et al. [23]. To examine the purity and subunit composition of the 20S proteasomes, aliquots were subjected to SDS-PAGE and non-denaturing PAGE. This preparation yielded more than eight typical bands of 20S proteasomes on SDS-PAGE and a single main band on the non-denaturing gel. Protein concentrations were measured using the method of Bradford [24].

Supported bilayers of lipid membranes were prepared using the Langmuir–Blodgett method [25]. We used a moving-wall-type Langmuir–Blodgett trough; i.e., the Bio-Trough (NL-BIO40-MWC) (Nippon Laser and Electronics Lab., Nagoya, Japan) [26]. Lipid monolayer membranes at the air–water interface were prepared by spreading lipid solution in hexane/ethanol (9:1, [v/v]). The first monolayers on freshly cleaved mica were prepared by transferring the monolayer membrane at the air–water interface to the mica surface attached to the slide glass, using the vertical method at constant surface pressure: 40 mN/m for DPPC monolayer, and 30 mN/m for SOPC monolayer. After drying in air for 30 min, the mica-supported monolayer membrane was glued to a Teflon-coated stainless disk (diameter, 14 mm) using a rapid epoxy glue. Then, the second monolayer was transferred to the monolayer on the mica using the horizontal method [25,27]. The resulting supported bilayer on mica was kept under water in a small container, and, during its transfer to the AFM liquid cell, it was kept under water.

We used a Nanoscope IIIa Multimode AFM (MMAFM) instrument (Digital Instruments, Santa Barbara, USA) equipped with a J scanner ($125 \times 125 \times 5.0$ μm) that was calibrated on a standard grid, and a fluid cell with an O-ring [19]. We used an oxide-sharpened Si_3N_4 tip mounted on a cantilever (NP-S; Digital Instruments) with a spring constant of $k = 0.06$ N/m for the contact mode, and $k = 0.12$ N/m for the tapping mode. In the contact mode, the force between the tip and a sample was kept at the lowest possible values (usually less than 200 pN) by continuously adjusting the set point during the imaging. In the tapping mode, the cantilever oscillation was tuned to a frequency between 5 and 9 kHz, and, to minimize the force between the tip and a sample, the free amplitude of the tip was 10–20 nm and the feedback was set to 90–95% of the free amplitude. AFM images were plane-fitted and flattened.

Contact AFM showed that the supported lipid bilayer of DPPC membrane had a flat surface with some defects (Fig. 1a). The difference in height between the bilayer surface and the defects was 5.7 ± 0.3 nm, which is equal to the membrane thickness of the supported DPPC bilayer, assuming that the surface in the defect is the mica surface. This corresponds to the gel-phase bilayer [17]. Tapping AFM (in 5 mM Tris–HCl [pH 7.5] and 150 mM NaCl) of the supported liquid-crystalline (Lα) phase bilayer of SOPC membrane shows that it had a uniform flat surface; it was difficult to detect defects because the two-dimensional diffusion coefficient of lipids in the Lα phase membrane is large (Fig. 1b) [17]. However, a few defects were detected, and the membrane thickness of the supported SOPC bilayer was determined to be 4.7 ± 0.5 nm. In a hybrid bilayer, in which a 20 mol% DOTAP/80 mol% SOPC monolayer (outer monolayer) was deposited on DPPC monolayer-coated mica (20% DOTAP/80% SOPC – DPPC), a uniform flat surface with a few defects was observed in the tapping AFM image (Fig. 1c). A cross-section of the line drawn in Fig. 1c shows that, in the 20% DOTAP/80% SOPC – DPPC bilayer, there were two membrane thicknesses: 3.9 ± 0.5 nm and 5.7 ± 0.5 nm (Fig. 1d).

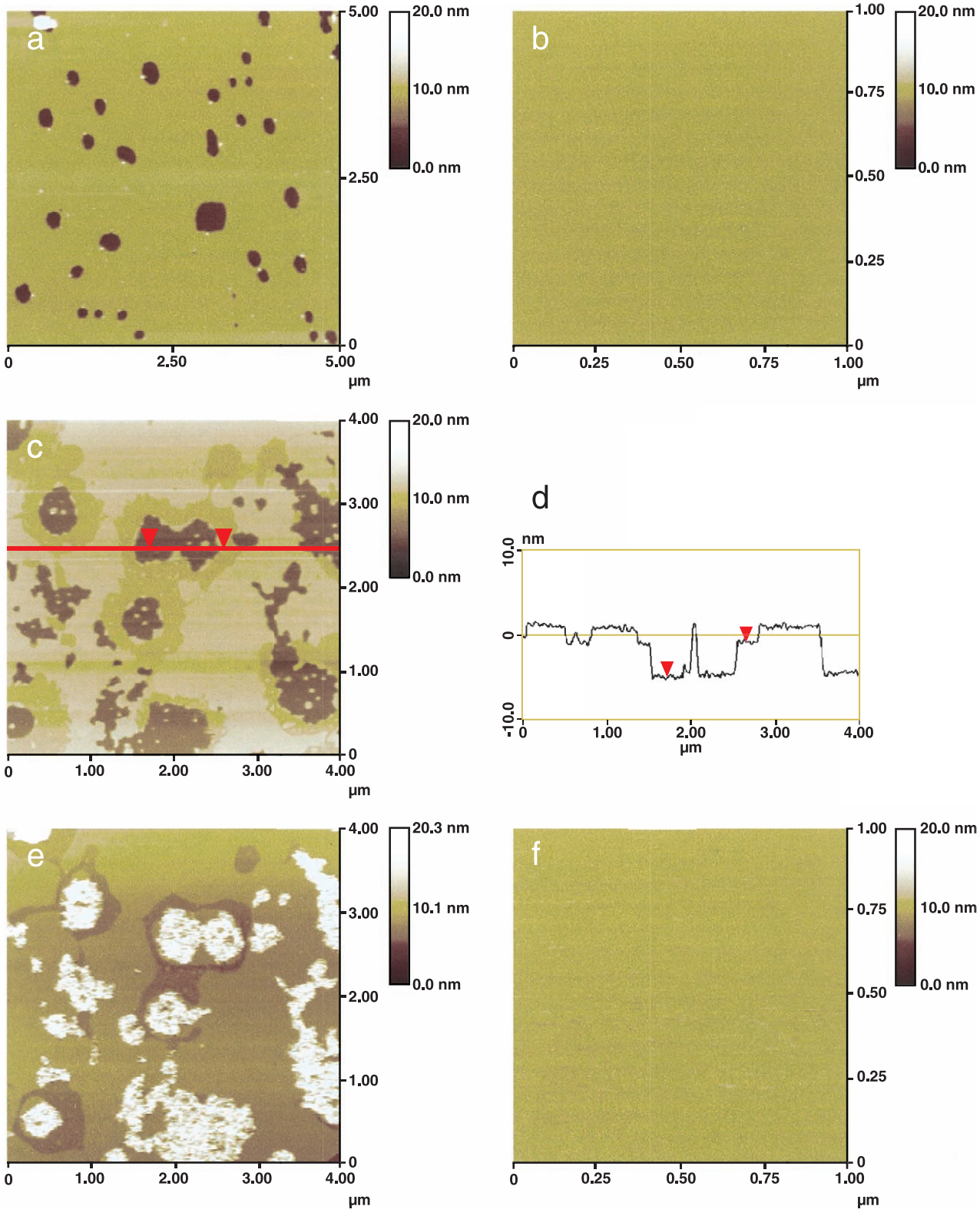

Fig. 1. Typical AFM images of supported bilayers on a mica. (a) DPPC bilayer observed in water. (b) SOPC bilayer observed in 5 mM Tris–HCl (pH 7.5), 150 mM NaCl. (c) 20% DOTAP/80% SOPC – DPPC bilayer in 5 mM Tris–HCl (pH 7.5), 150 mM NaCl. (d) A cross-section of the line drawn in panel c. Two arrows correspond to the positions indicated in panel c. (e) Interaction of the 20S proteasome with the 20% DOTAP/80% SOPC–DPPC bilayer (panel c) in 5 mM Tris–HCl (pH 7.5), 150 mM NaCl, 2 h incubation. (f) Interaction of the 20S proteasome with the SOPC bilayer (panel b) in 5 mM Tris–HCl (pH 7.5), 150 mM NaCl, 2 h incubation.

Considering the composition of the outer leaflet membrane (20% DOTAP/80% SOPC) and the length of the lipids, we can reasonably conclude that a membrane with a thickness of 3.9 nm and a membrane with a thickness of 5.7 nm correspond to the DOTAP – DPPC hybrid bilayer and the SOPC – DPPC hybrid bilayer, respectively. This indicates that phase separation occurred in the outer monolayer of the 20% DOTAP/80% SOPC – DPPC bilayer.

It was previously reported that the 20S proteasome was randomly adsorbed to mica [28]. However, when the 20S proteasome (final concentration, 11 μg/ml) was added to the buffer covering the supported SOPC bilayer, followed by incubation at room temperature (23 ± 2 °C) for 0.5 to 4 h, we did not observe proteins on the SOPC bilayer using tapping AFM (Fig. 1f). This result is consistent with those for many water-soluble proteins; they are easily adsorbed onto mica, but not onto the phospholipid membranes [17,29].

To investigate effects of electrostatic interaction between the supported phospholipid bilayer and the 20S proteasome, we first prepared supported positively charged bilayers (20% DOTAP/80% SOPC – DPPC membranes) on mica (Fig. 1c), and investigated binding of the 20S proteasome to the bilayer using tapping AFM. When the 20S proteasome (final concentration, 11 μg/ml) was added to the buffer covering the supported bilayer, followed by incubation at 23 ± 2 °C for 0.5–4 h, we did not find proteins on the surface of the 20% DOTAP/80% SOPC–DPPC membrane, but many 20S proteasomes were observed in the defects of the bilayer; i.e., on the mica surface (Fig. 1e). This indicates that the 20S proteasome did not bind to the positively charged bilayer. Then, we prepared supported negatively charged bilayers (10% DOPA/90% DOPC – DPPC membranes) on mica, and investigated binding of the 20S proteasome to these bilayers. The result was almost the same as that of the 20% DOTAP/80% SOPC – DPPC membrane, indicating that the 20S proteasome did not bind to the negatively charged bilayer containing DOPA.

Finally, we investigated the effects of specific interaction between the lipid (PI) and the 20S proteasome. We prepared a supported hybrid bilayer of a 50% PI/50% SOPC – SOPC membrane, and its tapping AFM image shows that the hybrid bilayer had a uniform flat surface (Fig. 2a). When the 20S proteasome was added to the buffer covering the supported 50% PI/50% SOPC – SOPC bilayer, followed by incubation at 23 ± 2 °C for 30 min, many particles were observed in the AFM image (Fig. 2b), indicating that the 20S proteasomes bound to the supported bilayer. The number of 20S proteasomes bound to the bilayer increased with increasing time; after 4 h, the binding became saturated (Fig. 2b–d).

To observe the 20S proteasome on the supported bilayer with higher resolution, we tried to prepare a two-dimensional crystal of the 20S proteasome on a supported bilayer containing PI. For this purpose, we prepared a supported 20% PI/80% SOPC – SOPC bilayer, because the lower density of the receptor (i.e., PI) of the protein readily undergoes two-dimensional crystallization. Fig. 2e shows an AFM image (field, 500 × 500 nm) of the 20S proteasomes on the supported 20% PI/80% SOPC – SOPC bilayer, after incubation for 24 h at 23 ± 2 °C, and indicates that many 20S proteasomes bound to the supported bilayer at high density, although we could not get a high-quality two-dimensional crystal of the 20S proteasome. A magnified AFM image (Fig. 2f) shows that the 20S proteasomes had a nearly circular shape with an average diameter of 10 ± 2 nm. Previously, high-resolution X-ray crystal analysis has shown that the overall structure of eukaryotic 20S proteasomes is a cylinder with a diameter of 11–12 nm and a length of 15–17 nm in the side view position [7–9]. Thus, the present AFM results show that 20S proteasomes on the supported 20% PI/80% SOPC – SOPC bilayer are in an "upright" orientation, or in a top view position, with their α-rings on the top and bottom. Almost all 20S proteasomes on this supported bilayer were in the "upright" orientation. This is in contrast to previous observations of 20S proteasomes on mica, in which only a third of the protein assemblies were in the "upright" orientation [28]. Very recently, recombinant 20S proteasome His-tagged at their ends were observed to form a two-dimensional crystal on a nickel-chelating lipid membrane, and their images on AFM were almost circular with a diameter of 11 nm, indicating that the 20S proteasomes were in a top view position [30]. This finding supports our conclusion that the 20S proteasomes were in the "upright" orientation.

The present AFM study of interactions of the 20S proteasome with supported bilayers of various lipids in a buffer clearly indicates that the 20S proteasomes can strongly bind to lipid membranes containing PI in the "upright" orientation, but cannot bind to membranes of other lipids such as PC, PA and DOTAP. The specific binding of PI with the 20S proteasome may play an important role in the binding of 20S proteasomes on biomembranes in cells. For instance, the ER membrane contains abundant PI molecules [31,32], and the 20S proteasome may bind to the ER membrane via PI. Moreover, the present results show that use of AFM to study supported bilayers in a buffer provides new information on ligand–receptor interaction.

Fig. 2. Interaction of the 20S proteasome with PI/SOPC – SOPC bilayers in 5 mM Tris–HCl (pH 7.5), 150 mM NaCl. (a) A typical AFM image of a supported hybrid bilayer of the 50% PI/50% SOPC – SOPC membrane before the 20S proteasome was added. (b) An AFM image of the same bilayer (panel a) after 30 min incubation with the 20S proteasome. (c) After 140 min incubation. (d) After 4 h incubation. (e) A high-resolution image of the 20S proteasome on the 20% PI/80% SOPC – SOPC membrane after 24 h incubation with the 20S proteasome. (f) A magnified image of panel e. Scale bar is 10 nm.

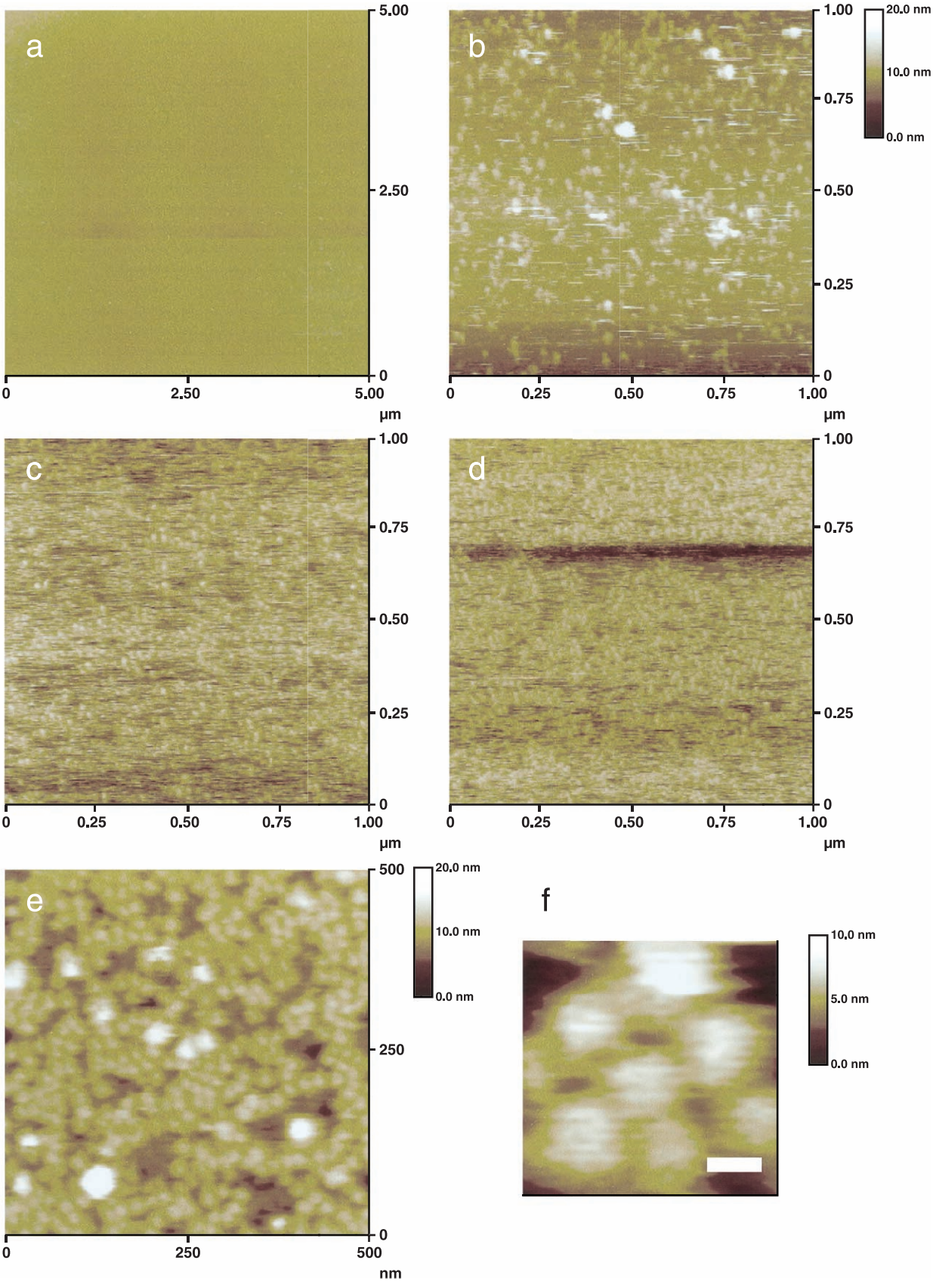
a
5.00
2.50
0
0
2.50
5.00
μm
b
1.00
0.75
0.50
0.25
0
0
0.25
0.50
0.75
1.00
μm
20.0 nm
10.0 nm
0.0 nm
c
1.00
0.75
0.50
0.25
0
0
0.25
0.50
0.75
1.00
μm
d
1.00
0.75
0.50
0.25
0
0
0.25
0.50
0.75
1.00
μm
e
500
250
0
0
250
500
nm
20.0 nm
10.0 nm
0.0 nm
f
10.0 nm
5.0 nm
0.0 nm

Acknowledgements

This work was supported in part by a Grant-in-Aid for General Scientific Research C from the Ministry of Education, Science, and Culture (Japan) to M.Y.

References

[1] O. Coux, K. Tanaka, A.L. Goldberg, Ann. Rev. Biochem. 65 (1996) 801–847.
[2] W. Baumeister, J. Walz, F. Zühl, E. Seemüller, Cell 92 (1998) 367–380.
[3] B. Tsai, Y. Yihong, T.A. Rapoport, Nat. Rev., Mol. Cell Biol. 3 (2002) 246–255.
[4] L. Ellgaard, A. Helenius, Nat. Rev., Mol. Cell Biol. 4 (2003) 181–191.
[5] C. Hirsch, H.L. Ploegh, Trends Cell Biol. 10 (2000) 268–272.
[6] W. Baumeister, Z. Cejka, M. Kania, E. Seemuller, Biol. Chem. 378 (1997) 121–130.
[7] J. Lowe, D. Stock, B. Jap, P. Zwickl, W. Baumeister, R. Huber, Science 268 (1995) 533–539.
[8] M. Groll, L. Ditzel, J. Lowe, D. Stock, M. Bochtler, H.D. Bartunik, R. Huber, Nature 386 (1997) 463–471.
[9] M. Unno, T. Mizushima, Y. Morimoto, Y. Tomisugi, K. Tanaka, N. Yasuoka, T. Tsukihara, J. Biochem. 131 (2002) 171–173.
[10] K. Tanaka, T. Yoshimura, A. Ichihara, J. Biochem. 106 (1989) 495–500.
[11] I. Ruiz de Mena, E. Mahillo, J. Arribas, J.G. Castano, Biochem. J. 296 (1993) 93–97.
[12] S. Yamada, K. Hojo, H. Yoshimura, K. Ishikawa, J. Biochem. 117 (1995) 1162–1169.
[13] N. Watanabe, S. Yamada, Plant Cell Physiol. 37 (1996) 147–151.
[14] S. Yamada, K. Sato, M. Uritani, T. Tokumoto, K. Ishikawa, Biosci. Biotechnol. Biochem. 62 (1998) 1264–1266.
[15] R.H. Newman, P. Whitehead, J. Lally, A. Coffer, P. Freemont, Biochim. Biophys. Acta 1281 (1996) 111–116.
[16] H.G. Hansma, J. Hoh, Annu. Rev. Biophys. Biomol. Struct. 23 (1994) 115–128.
[17] J. Mou, J. Yang, Z. Shao, J. Mol. Biol. 248 (1995) 507–512.
[18] S. Scheuring, D.J. Müller, P. Ringler, J.B. Heymann, A. Engel, J. Microscopy 193 (1999) 28–35.
[19] S. Furuike, T. Ito, M. Yamazaki, FEBS Lett. 498 (2001) 72–75.
[20] T. Ando, N. Kodera, E. Takai, D. Maruyama, K. Saito, A. Toda, Proc. Natl. Acad. Sci. U. S. A. 98 (2001) 12468–12472.
[21] I. Reviakine, A. Brisson, Langmuir 17 (2001) 8293–8299.
[22] S. Furuike, S. Yamada, M. Yamazaki, Biophys. Jpn. 42S (2002) 63.
[23] C.P. Ma, C.A. Slaughter, G.N. DeMartino, J. Biol. Chem. 267 (1992) 10515–10523.
[24] M.M. Bradford, Anal. Biochem. 72 (1976) 249–254.
[25] G. Roberts, Langmuir–Blodgett Films, Plenum, New York, 1990.
[26] H. Kumehara, T. Kasuga, T. Watanabe, S. Miyata, Thin Solid Films 178 (1989) 175–182.
[27] V. Tscharner, H.M. McConnell, Biophys. J. 36 (1981) 421–427.
[28] P.A. Osmulski, M. Gaczynska, J. Biol. Chem. 275 (2000) 13171–13174.
[29] J. Yang, J. Mou, Z. Shao, Biochim. Biophys. Acta 1199 (1994) 105–114.
[30] A. Thess, S. Hutschenreiter, M. Hofmann, R. Tampe, W. Baumeister, R. Guckenberger, J. Biol. Chem. 277 (2002) 36321–36328.
[31] J. Vidugiriene, D.K. Sharma, T.K. Smith, N.A. Baumann, A.K. Menon, J. Biol. Chem. 274 (1999) 15203–15212.
[32] R.O. Calderon, G.H. DeVries, J. Neurosci. Res. 49 (1997) 372–380.